Modelling of 12-DoF Parachute - Riser - Payload System Dynamics using Kane's method

Prashant G Iyer (prashant_gi@vssc.gov.in)
Vikram Sarabhai Space Centre

Research Article

Keywords: Multi-body dynamics, Parachute Riser Payload System, Kane's method, generalized coordinates, Parachute opening transients, Equations of motion

Posted Date: March 27th, 2023

DOI: https://doi.org/10.21203/rs.3.rs-2728306/v1

Additional Declarations: No competing interests reported.

Modelling of 12-DoF Parachute - Riser - Payload System Dynamics using Kane's method

Prashant G. Iyer

Received: date / Accepted: date

Abstract Dynamic behaviour of parachutes is highly complex and characterised by non-linear, time dependant Fluid Structure Interaction, which is computationally intensive and hence not a viable option for incorporating into trajectory simulations. The paper describes modelling of "Computationally efficient, High Fidelity Multi-Body" Parachute - Elastic Riser - Payload system, capable of simulating trajectory from parachute deployment to parachute separation. The differential equations of motion, including the kinematical and kinetic relationships are derived using the matrix form of Kane's method, which avoids the typical complexity involved in symbolic derivations, available in published literature. The developed model is validated with published literature results formulated using Newton Euler method and simulation results demonstrating the typical characteristic motion of the system during descend are presented.

Keywords Multi-body dynamics · Parachute Riser Payload System · Kane's method · generalized coordinates · Parachute opening transients · Equations of motion

1 Introduction

Parachute systems are widely used in various fields nowadays, such as spacecraft recovery, planet probe landing and rapid aerial delivery of equipment and supplies [10]. A typical deceleration system for spacecraft recovery consists of clustered parachute system comprising of different kinds of parachutes, which deploy in a predetermined sequence to bring down the velocity of spacecraft to safe levels at the instance of splash-down whilst maintaining the stability of the system.

Available literature like Fallon(1991) [2], Guglieri(2012) [4], Ibrahim and Engdahl(1974) [8] and Paul et al.(2016) [13], have modelled multi-body Parachute Payload system using Newton-Euler method with varying degrees of freedom and validated their model with actual flight data. But this formulation involves deriving the internal constraint forces, which tends

Prashant G. Iyer
Vikram Sarabhai Space Centre, Thiruvananthapuram, Kerala - 695022, India
Tel.: +91-8113857704
E-mail: prashant_gi@vssc.gov.in

to become tedious when the complexity of system increases, as in case with multi-chute system. Analytical methods like Euler-Lagrange method on the other hand requires calculating the derivatives of a scalar Lagrange term, which can be very complex for large systems and can lead to the issue of *intermediate swell* as reported by Duan(2006) [1]. Kane's method is extensively used in the literature to model multi-body systems, attributable to its use of generalized speeds. It results in a simplistic vectorial form of equations of motion involving partial velocity and accelerations, describing the system on a whole and eliminating the need of deriving constraint forces and moments. Stoneking(2013) [15] has presented an alternative matrix form of Kane's equation which is amenable to be used numerically, facilitating the modelling of multiple interconnected bodies. But, matrix expressions to model variable mass systems is not provided, which has been adressed in this paper.

Ke et al.(2009) [10] presented an algorithm to model and simulate the general parachute-payload system including the parachute opening transients and contact forces, using the analytical form of Kane's equation. This paper describes the modelling of a Parachute Riser Payload System (PRPS) consisting of rigid payload and rigid parachute linked using an elastic riser having a non-zero mass using matrix form of Kane's equation. This high fidelity model is capable of simulating the parachute dynamics from parachute deployment till parachute separation, including the parachute opening transients where the PRPS acts as a constant mass system with variable mass bodies. Analytical expressions for fore-body wake effects and energy modifications due to apparent mass have also been included to make the model more realistic.

1.1 Notations

The notations used in this paper for representation of vector quantities in different reference frames are stated below, following the standards used in Pal(2020) [12].

- ${}^{B}C^{A}$ denotes the Direction Cosine matrix of frame A with respect to frame B.
- ${}^{C}\vec{\omega}^{A/B}$ and ${}^{C}\vec{\alpha}^{A/B}$ denote the angular velocity and angular acceleration respectively of frame A with respect to frame B expressed in frame C.
- ${}^{C}\vec{r}^{p/o}$, ${}^{C}\vec{v}^{p/o}$ and ${}^{C}\vec{a}^{p/o}$ denote the position, linear velocity and acceleration vectors of the point p from point o expressed in the frame C.
- ${}^{A}\vec{F}^{B}_{name}$ is the force vector identified with *name* acting on body B expressed in the frame A.
- The moment vector denoted as ${}^{A}\vec{M}^{B/o}_{name}$, is the moment vector identified with *name* acting on body B about the point o, expressed in the frame A.

2 Kane's Method for Variable Mass Systems

Hurtado(2018) [7] derived the Lagrange-Cayley equations for variable mass systems from first principles, considering the kinematic relationships due to mass variations. For a variable mass multibody system, consisting of N_b rigid bodies with n degrees of freedom, the system dynamics in Kane's form is developed as a set of scalar equations following Kane

and Levison(1985) [9], extended from Hurtado formulation using d'Alembert principle.

$$\begin{aligned}
&\sum_{k=1}^{N_b}\left[\vec{\omega}_r^k\cdot\left(\vec{M}_k - I_k\vec{\alpha}_k - \dot{I}_k\vec{\omega}_k - \vec{\omega}_k\times I_k\vec{\omega}_k\right)\right]\\
&+\sum_{k=1}^{N_b}\left[\vec{v}_r^k\cdot\left(\vec{F}_k - m_k\vec{a}_k - \dot{m}_k\vec{v}_k\right)\right]\\
&+\sum_{k=1}^{N_b}\left[\sum_j\left(\vec{v}_{r,j}^k\cdot\left(\vec{f}_{j,k} - \dot{m}_{j,k}\vec{v}_{j,k}\right)\right)\right] = 0,\\
&\qquad\qquad\qquad\qquad\qquad\qquad\qquad\qquad r = 1,2,\ldots,n
\end{aligned} \tag{1}$$

where $\vec{M}_k$ and $\vec{F}_k$ are the active moments and forces acting on k^{th} body respectively. $\vec{\omega}_r^k$ and $\vec{v}_r^k$ are the partial angular velocity and partial linear velocity of the k^{th} body with respect to the r^{th} generalized speed. $\vec{\alpha}_k$ and $\vec{\omega}_k$ are the angular acceleration and angular velocity of the k^{th} body about its CG, and $\vec{a}_k$ and $\vec{v}_k$ are the respective linear acceleration and linear velocity of the CG. m_k defines the mass, and I_k defines inertia tensor of the k^{th} body in its own body axis with respect to the CG. $\vec{v}_{r,j}^k$ is the partial linear velocity of the ejected mass from j^{th} ejection location of k^{th} body with respect to the r^{th} generalized speed, $\vec{f}_{j,k}$ is the force acting on the j^{th} ejected mass from k^{th} body and $\vec{v}_{j,k}$ is the inertial velocity of the j^{th} ejected mass from k^{th} body.

Stoneking(2013) [15] styled the matrix form of Kane's formulation for a constant mass rigid body system. This is extended to include variable mass effects, consistent with Equation 1 as

$$\begin{aligned}
\left(\Omega^T[I]\Omega + V^T[m]V\right)\dot{u} =\\
\Omega^T\left(\{M\} - [I]\{\alpha_r\} - [\dot{I}]\{\omega\} - \{\omega\}\times[I]\{\omega\}\right)\\
+V^T\left(\{F\} - [\dot{m}]\{v\} - [m]\{a_r\}\right)\\
+V_{EJ}^T\left(\{F_{EJ}\} - [\dot{M_{EJ}}]\{v_{EJ}\}\right)
\end{aligned} \tag{2}$$

where, Ω and V are the partial angular and linear velocity matrices, α_r and a_r are the remainder angular acceleration and linear acceleration respectively, ω and v are the angular velocity and linear velocity vectors, F and M are the multi-body force and moment matrices, m and I are the multi-body mass and inertia matrixces and $\vec{u}$ is the column matrix of the generalized speeds. V_{EJ} represents the partial linear ejection velocity matrix, F_{EJ} is the ejected mass force matrix and M_{EJ} is the generalized multibody ejection mass matrix.

V_{EJ} defined in Equation 2 is a 3 dimensional array, which can result in computationally intensive multiplication operation. Hence, a generalized reaction thrust generated as a direct consequence of mass variation is added in $\vec{M}_k$ and $\vec{F}_k$ matrices, as described in Ge et al.(1982) [3], simplifying Equation 2 as

$$\begin{aligned}
\left(\Omega^T[I]\Omega + V^T[m]V\right)\dot{u} =\\
\Omega^T\left(\{M\} - [I]\{\alpha_r\} - [\dot{I}]\{\omega\} - \{\omega\}\times[I]\{\omega\}\right)\\
+V^T\left(\{F\} - [\dot{m}]\{v\} - [m]\{a_r\}\right)
\end{aligned} \tag{3}$$

3 Mathematical Modelling

3.1 Modelling of Parachute Riser Payload System

The 3-body PRPS presented in this paper is illustrated in Fig. 1, with O_1, O_2 and O_3 being the CG's of payload, riser and parachute respectively. An elastic riser is attached to the payload (at *riser attachment point*) on one end using a universal joint J_1 and to the parachute (at *parachute confluence point*) on other end with a spherical joint J_2. From J_2, the suspension lines of the parachute fork out, with a semi oblate spheriod canopy attached to it, forming the rigid body parachute.

The following assumptions are considered while modelling the PRPS:

- The aerodynamic forces generated by suspension lines and riser are considered negligible.
- The forces resulting from twisted risers and distortion of the shape of the parachute canopies are neglected.
- The aerodynamic centres of pressure remain on the axes of symmetry of the vehicle and the parachute, but do not necessarily coincide with the centre of mass those bodies.
- Trajectory simulations are carried out considering flat earth assumption.

3.2 Coordinate Frames

The reference frames used in modelling the PRPS, as illustrated in Fig. 1, are described below:

- Inertial reference frame N (X_N, Y_N, Z_N) - This Newtonian reference frame is selected as Launch Point Inertial (LPI) frame. The origin is fixed at time $t = 0$ on the Earth's surface directly below the Payload CG. The X_N axis is along the local vertical pointing away from the ground, Z_N lies in the horizontal plane making an angle ψ_L with local north and Y_N axis completes the right-handed coordinate system.
- B_1 frame (X_{B1}, Y_{B1}, Z_{B1}) - This reference frame is attached to the Payload at its CG O_1. The X_{B1} axis is along the longitudinal axis and positive towards apex cover, Z_{B1} axis is in the horizontal plane and pointing towards the hatch and Y_{B1} axis completes the right-handed coordinate system.
- B_2 frame (X_{B2}, Y_{B2}, Z_{B2}) - This reference frame is attached to the riser at its CG O_2 with the X_{B2} axis along the length of the riser pointing towards parachute confluence point J_2.
- B_3 frame (X_{B3}, Y_{B3}, Z_{B3}) - The reference frame is attached to the Parachute at its CG O_3. The X_{B3} axis is along the longitudinal axis of the parachute pointing towards the canopy.

3.3 Vector of Generalized Coordinates and Speeds

The degrees of freedom for this multi-body system is designated as.

- Payload is represented as a rigid body having 6 degrees of freedom - 3 translational degrees of freedom in the inertial space, given by ${}^N\vec{r}_0 = (x_0, y_0, z_0)$ and 3 rotational degrees of freedom about the CG O_1, denoted by rotation angle θ_{pay}, ψ_{pay} and ϕ_{pay}.

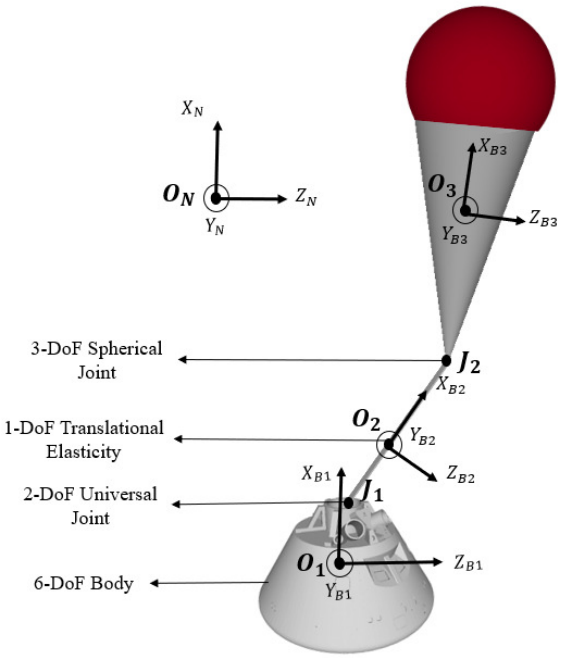

Fig. 1: Illustration of Coordinate frames and 12-DoF PRPS model

Following the rotation sequence $Y \rightarrow Z \rightarrow X$ the transformation from N frame to B_1 frame is represented by

$$N \xrightarrow[\text{by } \theta_{pay}]{\text{about } Y} B_1' \xrightarrow[\text{by } \psi_{pay}]{\text{about } Z} B_1'' \xrightarrow[\text{by } \phi_{pay}]{\text{about } X} B_1$$

– The riser B_2 has 2 rotational degrees of freedom about the joint J_1, denoted by the joint angles θ_{riser} and ψ_{riser} and 1 translational degree of freedom due to its elastic property i.e. L_{riser}. Following the rotation sequence $Y \rightarrow Z$ the transformation from B_1 frame to B_2 frame is represented by

$$B_1 \xrightarrow[\text{by } \theta_{riser}]{\text{about } Y} B_2' \xrightarrow[\text{by } \psi_{riser}]{\text{about } Z} B_2$$

– Parachute B_3 is considered a rigid body having 3 rotational degrees of freedom about the joint J_2, denoted by the joint angles θ_{par}, ϕ_{par} and ψ_{par}. Following the rotation sequence $Y \rightarrow X \rightarrow Z$, the transformation from B_2 frame to B_3 frame is represented by

$$B_2 \xrightarrow[\text{by } \theta_{par}]{\text{about } Y} B_3' \xrightarrow[\text{by } \phi_{par}]{\text{about } X} B_3'' \xrightarrow[\text{by } \psi_{par}]{\text{about } Z} B_3$$

Based on the 12 degrees of freedom of the system, the selected generalized speeds is represented as a column vector as follows:

$$\vec{u} = [\vec{\omega}_1, \sigma_2, \sigma_3, \vec{v}_1, \dot{L}_{riser}]^T \tag{4}$$

where,

$$\vec{\omega}_1 = \begin{Bmatrix} p_{pay} \\ q_{pay} \\ r_{pay} \end{Bmatrix}, \quad \sigma_2 = \begin{Bmatrix} \dot{\theta}_{riser} \\ \dot{\psi}_{riser} \end{Bmatrix}, \quad \sigma_3 = \begin{Bmatrix} \dot{\theta}_{par} \\ \dot{\phi}_{par} \\ \dot{\psi}_{par} \end{Bmatrix}, \quad \vec{v}_1 = \begin{Bmatrix} \dot{x}_0 \\ \dot{y}_0 \\ \dot{z}_0 \end{Bmatrix}$$

3.4 Derivation of Equations of Motion

The transformation matrices between the various frames is computed from the described Euler angle sequences in section 3.3, using methodology as mentioned in Henderson(1977) [6].

The relative angular body rates of each of the bodies can be represented in terms of the joint angular rates (σ) using the system kinematics.

$$^{B1}\vec{\omega}^{B1/N} = \vec{\omega}_1 \tag{5a}$$

$$^{B2}\vec{\omega}^{B2/B1} = \Gamma_2 \sigma_2 \tag{5b}$$

$$^{B3}\vec{\omega}^{B3/B2} = \Gamma_3 \sigma_3 \tag{5c}$$

where,

$$\Gamma_2 = \begin{bmatrix} \sin\psi_{riser} & 0 \\ \cos\psi_{riser} & 0 \\ 0 & 1 \end{bmatrix}, \Gamma_3 = \begin{bmatrix} \cos\phi_{par}\sin\psi_{par} & \cos\psi_{par} & 0 \\ \cos\phi_{par}\cos\psi_{par} & -\sin\psi_{par} & 0 \\ -\sin\phi_{par} & 0 & 1 \end{bmatrix} \tag{6}$$

The angular velocities of the 3 bodies B_1, B_2 and B_3 with respect to the inertial N frame expressed in their respective body frames can be derived as:

$$^{B1}\vec{\omega}^{B1/N} = \vec{\omega}_1 \tag{7a}$$

$$\begin{aligned} ^{B2}\vec{\omega}^{B2/N} &= {}^{B2}C^{B1B1}\vec{\omega}^{B1/N} + {}^{B2}\vec{\omega}^{B2/B1} \\ &= {}^{B2}C^{B1}\omega_1 + \Gamma_2\sigma_2 \end{aligned} \tag{7b}$$

$$\begin{aligned} ^{B3}\vec{\omega}^{B3/N} &= {}^{B3}C^{B2B2}\vec{\omega}^{B2/N} + {}^{B3}\vec{\omega}^{B3/B2} \\ &= {}^{B3}C^{B1}\omega_1 + {}^{B3}C^{B2}\Gamma_2\sigma_2 + \Gamma_3\sigma_3 \end{aligned} \tag{7c}$$

Equation (7) can be grouped together into a system of identities to form the *partial angular velocity matrix* Ω.

$$\begin{bmatrix} ^{B1}\vec{\omega}^{B1/N} \\ ^{B2}\vec{\omega}^{B2/N} \\ ^{B3}\vec{\omega}^{B3/N} \end{bmatrix} = \underbrace{\begin{bmatrix} I_{3\times3} & 0_{3\times2} & 0_{3\times3} & 0_{3\times3} & 0_{3\times1} \\ {}^{B2}C^{B1} & \Gamma_2 & 0_{3\times3} & 0_{3\times3} & 0_{3\times1} \\ {}^{B3}C^{B1} & {}^{B3}C^{B2}\Gamma_2 & \Gamma_3 & 0_{3\times3} & 0_{3\times1} \end{bmatrix}}_{\Omega} \vec{u} \tag{8}$$

Subsequently, the angular acceleration of the each of the bodies B_i , $i = 1,2,3$ with respect to frame N expressed in their corresponding body frame can be derived, as mentioned in Pal(2020) [12]:

$$^{B1}\vec{\alpha}^{B1/N} = {}^{B1}\dot{\vec{\omega}}^{B1/N} \tag{9a}$$

$$^{B2}\vec{\alpha}^{B2/N} = {}^{B2}C^{B1B1}\dot{\vec{\omega}}^{B1/N} + \Gamma_2\dot{\sigma}_2 + {}^{B2}\vec{\alpha}_r^{B2/N} \tag{9b}$$

$$^{B3}\vec{\alpha}^{B3/N} = {}^{B3}C^{B1B1}\dot{\vec{\omega}}^{B1/N} + {}^{B3}C^{B2}\Gamma_2\dot{\sigma}_2 + \Gamma_3\dot{\sigma}_3 + {}^{B3}\vec{\alpha}_r^{B3/N} \tag{9c}$$

where ${}^{B2}\vec{\alpha}_r^{B2/N}$ and ${}^{B3}\vec{\alpha}_r^{B3/N}$ are the *remainder angular acceleration* following the terminology of Stoneking(2013) [15], and $\dot{\Gamma}_2$ and $\dot{\Gamma}_3$ are the time derivatives of Γ_2 and Γ_3 respectively.

$$ {}^{B2}\vec{\alpha}_r^{B2/N} = \dot{\Gamma}_2\sigma_2 + \left({}^{B2}C^{B1}\ \vec{\omega}_1\right) \times {}^{B2}\vec{\omega}^{B2/B1} \tag{10a} $$

$$ \dot{\Gamma}_2 = \begin{bmatrix} \dot{\psi}_{riser}\cos\psi_{riser} & 0 \\ -\dot{\psi}_{riser}\sin\psi_{riser} & 0 \\ 0 & 0 \end{bmatrix} \tag{10b} $$

$$ {}^{B3}\vec{\alpha}_r^{B3/N} = {}^{B3}\vec{\alpha}_r^{B2/N} + \dot{\Gamma}_3\sigma_3 + \left({}^{B3}\vec{\omega}^{B2/N}\right) \times {}^{B3}\vec{\omega}^{B3/B2} \tag{10c} $$

$$ \dot{\Gamma}_3 = \begin{bmatrix} -\dot{\phi}_{par}\sin\phi_{par}\sin\psi_{par} + \dot{\psi}_{par}\cos\phi_{par}\cos\psi_{par} & -\dot{\psi}_{par}\sin\psi_{par} & 0 \\ -\dot{\phi}_{par}\sin\phi_{par}\cos\psi_{par} - \dot{\psi}_{par}\cos\phi_{par}\sin\psi_{par} & -\dot{\psi}_{par}\cos\psi_{par} & 0 \\ -\dot{\phi}_{par}\cos\phi_{par} & 0 & 0 \end{bmatrix} \tag{10d} $$

Next, the position of the points O_1, J_1, O_2, J_2 and O_3 are derived with respect to n, a point fixed in the inertial frame N expressed in the inertial frame.

$$ {}^{N}\vec{r}^{O_1/n} = {}^{N}\vec{r}_0 \tag{11a} $$

$$ {}^{N}\vec{r}^{J_1/n} = {}^{N}\vec{r}^{O_1/n} + {}^{N}C^{B1B1}\vec{r}^{J_1/O_1} \tag{11b} $$

$$ {}^{N}\vec{r}^{O_2/n} = {}^{N}\vec{r}^{J_1/n} - {}^{N}C^{B2B2}\vec{r}^{J_1/O_2} \tag{11c} $$

$$ {}^{N}\vec{r}^{J_2/n} = {}^{N}\vec{r}^{O_2/n} + {}^{N}C^{B2B2}\vec{r}^{J_2/O_2} \tag{11d} $$

$$ {}^{N}\vec{r}^{O_3/n} = {}^{N}\vec{r}^{J_2/n} - {}^{N}C^{B3B3}\vec{r}^{J_2/O_3} \tag{11e} $$

where,

- ${}^{B1}\vec{r}^{J_1/O_1}$ is derived based on riser attachment point on the payload.
- ${}^{B2}\vec{r}^{J_1/O_2}$ and ${}^{B2}\vec{r}^{J_2/O_2}$ satisfy the following equation assuming that the riser has a uniform mass distribution

$$ \begin{bmatrix} \frac{L_{riser}}{2} \\ 0 \\ 0 \end{bmatrix} = -{}^{B2}\vec{r}^{J_1/O_2} = {}^{B2}\vec{r}^{J_2/O_2} \tag{12} $$

- ${}^{B3}\vec{r}^{J_2/O_3}$ is worked out based on the Parachute center of mass, which has been derived as per Ibrahim and Engdahl(1974) [8] assuming the parachute canopy as a semi-oblate spheriod with height h, radius r and mass m_C, and suspension lines having length L_s and mass m_L.

$$ {}^{B3}\vec{r}^{J_2/O_3} = \begin{bmatrix} -L_{cm} \\ 0 \\ 0 \end{bmatrix} = \begin{bmatrix} -\frac{(m_L L_{cms})+(m_C L_1)+(m_I L_1)}{m_L+m_C+m_I} \\ 0 \\ 0 \end{bmatrix} \tag{13} $$

where, L_{cm} is center of mass of parachute which is derived considering the included mass of the canopy $m_I = \frac{2}{3}\rho\pi r^2 h$, density of atmosphere ρ and center of mass of suspension lines of parachute L_{cms}.

$$ L_{cms} = (0.5L_s\cos(\sin^{-1}(\frac{r}{L_s}))) \tag{14} $$

Now, the velocity of the CG's for each of the bodies expressed in the inertial frame N can be derived as in Equation (15). The angular velocities of the bodies can be expanded in terms of generalized speeds as mentioned in Equation (7) and then, Equation (15) can be grouped to form the *partial velocity matrix* V, derived in Equation (16).

$$
\begin{aligned}
{}^N\vec{v}^{O_1/n} &= \vec{v}_1 && \text{(15a)}\\
{}^N\vec{v}^{O_2/n} &= {}^N\vec{v}^{O_1/n} + \left({}^N\vec{r}^{O_1/O_2} \times {}^NC^{B1B1}\vec{\omega}^{B1/N}\right)\\
&\quad + \left({}^N\vec{r}^{J_1/O_2} \times {}^NC^{B2B2}\vec{\omega}^{B2/B1}\right) && \text{(15b)}\\
&\quad + {}^NC^{B2}\frac{\dot{L}_{riser}}{2}\\
{}^N\vec{v}^{O_3/n} &= {}^N\vec{v}^{O_1/n} + \left({}^N\vec{r}^{O_1/O_3} \times {}^NC^{B1B1}\vec{\omega}^{B1/N}\right)\\
&\quad + \left({}^N\vec{r}^{J_1/O_3} \times {}^NC^{B2B2}\vec{\omega}^{B2/B1}\right) + \left({}^N\vec{r}^{J_2/O_3} \times {}^NC^{B3B3}\vec{\omega}^{B3/B2}\right) && \text{(15c)}\\
&\quad + {}^NC^{B2}\dot{L}_{riser}
\end{aligned}
$$

$$
\begin{bmatrix} {}^N\vec{v}^{O_1/n} \\ {}^N\vec{v}^{O_2/n} \\ {}^N\vec{v}^{O_3/n} \end{bmatrix} = \underbrace{\begin{bmatrix} 0_{3\times3} & 0_{3\times2} & 0_{3\times3} & I_{3\times3} & 0_{3\times1} \\ {}^Nr_\times^{O_1/O_2}{}^NC^{B1} & {}^Nr_\times^{J_1/O_2}{}^NC^{B2}\Gamma_2 & 0_{3\times3} & I_{3\times3} & {}^NC^{B2}/2 \\ {}^Nr_\times^{O_1/O_3}{}^NC^{B1} & {}^Nr_\times^{J_1/O_3}{}^NC^{B2}\Gamma_2 & {}^Nr_\times^{J_2/O_3}{}^NC^{B3}\Gamma_3 & I_{3\times3} & {}^NC^{B2} \end{bmatrix}}_{V} \vec{u} \qquad \text{(16)}
$$

${}^Nr_\times^{J_1/O_2}$ and other similar terms in Equation (16) are skew-symmetric matrices of vectors, which equivalently perform cross product of the given vector with some other vector.

Next, the accelerations of the points O_1,O_2 and O_3, are expressed as

$$
\begin{aligned}
{}^N\vec{a}^{O_1/n} &= {}^N\dot{\vec{v}}_1 && \text{(17a)}\\
{}^N\vec{a}^{O_2/n} &= {}^N\vec{a}^{O_1/n}\\
&\quad + {}^NC^{B1B1}\dot{\vec{\omega}}^{B1/N} \times {}^N\vec{r}^{O_2/O_1}\\
&\quad + {}^NC^{B2}\Gamma_2\dot{\sigma}_2 \times {}^N\vec{r}^{O_2/J_1} && \text{(17b)}\\
&\quad + {}^N\vec{\omega}^{B2/N} \times {}^NC^{B2}\dot{L}_{riser}\\
&\quad + {}^N\vec{a}_r^{O_2/n}\\
{}^N\vec{a}^{O_3/n} &= {}^N\vec{a}^{O_1/n}\\
&\quad + {}^NC^{B1B1}\dot{\vec{\omega}}^{B1/N} \times {}^N\vec{r}^{O_3/O_1}\\
&\quad + {}^NC^{B2}\Gamma_2\dot{\sigma}_2 \times {}^N\vec{r}^{O_3/J_1}\\
&\quad + {}^NC^{B3}\Gamma_3\dot{\sigma}_3 \times {}^N\vec{r}^{O_3/J_2} && \text{(17c)}\\
&\quad + 2 \times {}^N\vec{\omega}^{B2/N} \times {}^NC^{B2}\dot{L}_{riser}\\
&\quad + {}^N\vec{a}_r^{O_3/n}
\end{aligned}
$$

where the *remainder acceleration* ${}^N\vec{a}_r^{O_2/n}$ and ${}^N\vec{a}_r^{O_3/n}$ are

$$\begin{aligned}{}^N\vec{a}_r^{O_2/n} = {}&{}^N C^{B2B2}\,{}^{B2}\vec{\alpha}_r^{B2/N} \times {}^N\vec{r}^{O_2/J_1} \\ &+ {}^N\vec{\omega}^{B1/N} \times \left({}^N\vec{\omega}^{B1/N} \times {}^N\vec{r}^{J_1/O_1}\right) \\ &+ {}^N\vec{\omega}^{B2/N} \times \left({}^N\vec{\omega}^{B2/N} \times {}^N\vec{r}^{O_2/J_1}\right)\end{aligned} \tag{18a}$$

$$\begin{aligned}{}^N\vec{a}_r^{O_3/n} = {}&{}^N\vec{a}_r^{O_2/n} \\ &+ {}^N C^{B2B2}\,{}^{B2}\vec{\alpha}_r^{B2/N} \times {}^N\vec{r}^{J_2/O_2} \\ &+ {}^N C^{B3B3}\,{}^{B3}\vec{\alpha}_r^{B3/N} \times {}^N\vec{r}^{O_3/J_2} \\ &+ {}^N\vec{\omega}^{B2/N} \times \left({}^N\vec{\omega}^{2/N} \times {}^N\vec{r}^{J_2/O_2}\right) \\ &+ {}^N\vec{\omega}^{B3/N} \times \left({}^N\vec{\omega}^{B3/N} \times {}^N\vec{r}^{O_3/J_2}\right)\end{aligned} \tag{18b}$$

$$\begin{aligned}{}^N\vec{\omega}^{B1/N} &= {}^N C^{B1\ B1}\,{}^{B1}\vec{\omega}^{B1/N} \\ {}^N\vec{\omega}^{B2/N} &= {}^N C^{B2\ B2}\,{}^{B2}\vec{\omega}^{B2/N} \\ {}^N\vec{\omega}^{B3/N} &= {}^N C^{B3\ B3}\,{}^{B3}\vec{\omega}^{B3/N}\end{aligned} \tag{18c}$$

The active forces and moments acting on the system are the gravitational force, aerodynamic forces and moments, and forces and moments due to elasticity of the riser. Furthermore, during the parachute deployment and inflation phase, an additional generalized thrust is also added to cater to the effects due to variable mass, as described in Ge et al.(1982) [3]. Following the expressions of the translational and rotational accelerations, the active forces are expressed in the inertial frame, while the active moments are expressed in the frames of the bodies on which they act, about their respective centres of gravity.
For body B_1 i.e. payload, the active forces and moments acting are

$${}^N\vec{F}^{B_1} = {}^N\vec{F}_G^{B_1} + {}^N\vec{F}_A^{B_1} + {}^N\vec{F}_S^{B_1} + {}^N\vec{F}_{JD}^{B_1} \tag{19a}$$

$${}^{B1}\vec{M}^{B_1/O_1} = {}^{B1}\vec{M}_A^{B_1/O_1} + {}^{B1}\vec{M}_S^{B_1/O_1} + {}^{B1}\vec{M}_{JD}^{B_1/O_1} \tag{19b}$$

For body B_2 i.e. riser, the active forces and moments acting are

$${}^N\vec{F}^{B_2} = {}^N\vec{F}_G^{B_2} \tag{20a}$$

$${}^{B2}\vec{M}^{B_2/O_2} = 0_{3\times 1} \tag{20b}$$

and for body B_3 i.e. parachute, they are

$${}^N\vec{F}^{B_3} = {}^N\vec{F}_G^{B_3} + {}^N\vec{F}_A^{B_3} + {}^N\vec{F}_S^{B_3} + {}^N\vec{F}_{GT}^{B_3} \tag{21a}$$

$${}^{B3}\vec{M}^{B_3/O_3} = {}^{B3}\vec{M}_A^{B_3/O_3} + {}^{B3}\vec{M}_S^{B_3/O_3} \tag{21b}$$

where, $\vec{F}_G$, $\vec{F}_A$, $\vec{F}_S$ and $\vec{F}_{JD}$ are the gravitational force, aerodynamic force, elastic spring force, and jet damping force respectively, and $\vec{M}_A$, $\vec{M}_S$ and $\vec{M}_{JD}$ are the aerodynamic moment, spring moment and jet damping moment respectively.

Under the assumption of flat Earth, the gravitational forces in the inertial frame N can be written as

$$ {}^{N}\vec{F}_{G}^{B_i} = \begin{Bmatrix} -m_i g \\ 0 \\ 0 \end{Bmatrix} \tag{22} $$

where, m_i is the mass of body B_i, $i = 1,2,3$, and g is the acceleration due to gravity.

The spring force caused by elasticity of the riser is computed in the riser body frame B_2 as

$$ {}^{B2}\vec{F}_{S}^{B_3} = -{}^{B2}\vec{F}_{S}^{B_1} = \begin{Bmatrix} K(\Delta L_{riser}) - \zeta \dot{L}_{riser} \\ 0 \\ 0 \end{Bmatrix} \tag{23} $$

where, K and ζ are the spring constant and damping constant for the elastic riser.

$\vec{F}_{GT}$ is the generalized thrust added to the parachute to cater to the variable mass effects during the deployment and inflation phase as described in Ke et al.(2009) [10], with the equation as

$$ {}^{B_3}\vec{F}_{GT}^{B_3} = \begin{Bmatrix} \dot{ml} \\ 0 \\ 0 \end{Bmatrix} \tag{24} $$

The aerodynamic forces and moments acting on the payload and the parachute CG's ($i = 1,3$) expressed in their corresponding body frames as:

$$ {}^{Bi}\vec{F}_{A}^{B_i} = \begin{Bmatrix} C_{A,i} Q_i S_i \\ C_{S,i} Q_i S_i \\ C_{N,i} Q_i S_i \end{Bmatrix}, \quad {}^{Bi}\vec{M}_{A}^{B_i/O_i} = \begin{Bmatrix} C_{RM,i} Q_i S_i L_i \\ C_{PM,i} Q_i S_i L_i \\ C_{YM,i} Q_i S_i L_i \end{Bmatrix} + {}^{Bi}r^{O_i/CP_i} \times {}^{Bi}\vec{F}_{A}^{B_i} \tag{25} $$

where S_i is the reference area, L_i is the reference length and Q_i is the dynamic pressure of the i^{th} body. Since, the payload acts as a forebody to the parachute, Q_{par} would not be the freestream dynamic pressure. Hence, a simplistic model as given in Peterson and Johnson(2013) [14] is incorporated to simulate the wake effects, which consists of empirical constants (a,k,m and n) proposed by Heinrich and Eckstrom(1963) [5].

$$ Q_{par} = Q_\infty \times \left(1 + \left(\frac{2}{r^2} \frac{D_1}{D_2} \left[1 - e^{D_2 r^2} + \frac{D_1}{4} e^{2D_2 r^2} - \frac{D_1}{4} \right] \right) \right) \tag{26} $$

where,

$$ D_1 = \frac{a}{(Z/D_B)^m} \qquad \text{and} \qquad D_2 = \frac{-1}{0.435 k^2 (Z/D_B)^{2n}} \tag{27} $$

To form the system of differential equations, Ω and V matrices are derived in Equations (8) and (16) respectively. The remaining terms $[m]$, $[I]$, $\{\omega\}$, $\{\alpha_r\}$, $\{a_r\}$, $\{F\}$ and $\{M\}$ are

derived as follows:

$$[m] = \begin{bmatrix} m_1 I_{3\times3} & 0 & 0 \\ 0 & m_2 I_{3\times3} & 0 \\ 0 & 0 & (m_3+m_{3A})I_{3\times3} \end{bmatrix}, \quad [I] = \begin{bmatrix} I^{B_1/O_1} & 0 & 0 \\ 0 & I^{B_2/O_2} & 0 \\ 0 & 0 & I^{B_3/O_3} \end{bmatrix} \tag{28a}$$

$$\{\omega\} = \begin{Bmatrix} {}^{B1}\vec{\omega}^{B1/N} \\ {}^{B2}\vec{\omega}^{B2/N} \\ {}^{B3}\vec{\omega}^{B3/N} \end{Bmatrix}, \quad \{\alpha_r\} = \begin{Bmatrix} {}^{B1}\vec{\alpha}_r^{B1/N} \\ {}^{B2}\vec{\alpha}_r^{B2/N} \\ {}^{B3}\vec{\alpha}_r^{B3/N} \end{Bmatrix}, \quad \{a_r\} = \begin{Bmatrix} {}^{N}\vec{a}_r^{O_1/n} \\ {}^{N}\vec{a}_r^{O_2/n} \\ {}^{N}\vec{a}_r^{O_3/n} \end{Bmatrix} \tag{28b}$$

$$\{F\} = \begin{Bmatrix} {}^{N}\vec{F}^{B_1} \\ {}^{N}\vec{F}^{B_2} \\ {}^{N}\vec{F}^{B_3} \end{Bmatrix}, \quad \{M\} = \begin{Bmatrix} {}^{B1}\vec{M}^{B_1/O_1} \\ {}^{B2}\vec{M}^{B_2/O_2} \\ {}^{B3}\vec{M}^{B_3/O_3} \end{Bmatrix} \tag{28c}$$

where, I^{B_1/O_1}, I^{B_2/O_2} and I^{B_3/O_3} are the inertia matrices in their body frames about the respective centres of gravity O_1, O_2 and O_3, and m_{3A} is the apparent mass of the parachute.

- m_{3A} is computed considering the potential flow around the semi oblate spheriod geometry of the canopy as described in Kidane(2009) [11]:

$$m_{3A} = \frac{\alpha_0}{2-\alpha_0}\frac{2}{3}\rho\pi r^2 h \tag{29a}$$

$$\alpha_0 = r^2 h \int_0^\infty \frac{d\lambda}{(h^2+\lambda)(r^2+\lambda)\sqrt{(h^2+\lambda)}} \tag{29b}$$

- I^{B_1/O_1} is the inertia tensor of the payload which is an input.
- I^{B_2/O_2} can be computed assuming riser to be a uniform cylindrical rod of infinitesimally small radius, which would result in

$$I^{B_2/O_2} = \begin{bmatrix} 0 & 0 & 0 \\ 0 & \frac{m_2 L_{riser}^2}{12} & 0 \\ 0 & 0 & \frac{m_2 L_{riser}^2}{12} \end{bmatrix} \tag{30}$$

- The Inertia tensor for the parachute i.e. I^{B_3/O_3} is derived as expressed in Ibrahim and Engdahl(1974) [8].

$$I^{B_3/O_3} = \begin{bmatrix} I_{xx} & 0 & 0 \\ 0 & I_{yy} & 0 \\ 0 & 0 & I_{zz} \end{bmatrix} \tag{31}$$

where,

$$\begin{aligned} I_{xx} = {} & \frac{1}{12} m_L L_s^2 \sin^2(\sin^{-1}(\frac{r}{L_s})) \\ & + \frac{2}{3} m_C r^2 \\ & + 0.063\rho R_0^5 \end{aligned} \tag{32a}$$

$$\begin{aligned} I_{zz} = I_{yy} = {} & \frac{1}{12} m_L L_s^2 \cos^2(\sin^{-1}(\frac{r}{L_s})) + m_L(L_{cms} - L_{cm})^2 \\ & + \frac{1}{3} m_C (h^2 + r^2) + m_{1A}(L_1 - L_{cm})^2 \\ & + m_{1A}(L_1 - L_{cm})^2 + 0.042\rho R_0^5 \end{aligned} \tag{32b}$$

All the above terms are finally assembled into Equation 3, to form the system of differential equations describing the dynamics of Parachute-Riser-Payload System.

4 Results and Validation

The numerical simulations of the formulated model are described in this section. The system of differential equations derived in Equation 3 is solved at each instant using the LU-decomposition solver implemented in C++ to get the generalized accelerations $\dot{\vec{u}}$. These are integrated using the Runge-Kutta 4th order scheme to obtain the generalized speeds $\vec{u}$ which involves the attitude and position of the payload and the joint angles for riser and parachute. The formulated model is validated by modelling the SRB parachute recovery system using Newton-Euler formulation as described in Ibrahim and Engdahl(1974) [8] and subjecting the system to a 20 deg pendulum disturbance at an altitude of 1800m and initial downward velocity of 60m/s. Furthermore, the reference literature assumes riser to be a massless body which transmits only axial forces to the attachment points, which has been modelled by forcing m_{riser} to be an extremely small value. Additionally, the literature also considers simulation starts at the time instance when the parachute is fully deployed and inflated. The simulation has been carried out assuming flat earth model and altitude based density variation considering the Indian Standard Atmosphere. Table 1 gives the system parameters used for validation.

Table 1: Parameters used in validation simulation

Parameters	Value
g	$9.80665\ \mathrm{m\cdot s^{-2}}$
m_1	69 321 kg
m_2	1×10^{-6} kg
m_3	2210.991 kg
m_C	1020.121 kg
m_L	1190.87 kg
$I_{xx}^{B_1/O_1}$	$2\,259\,151\ \mathrm{kg\cdot m^2}$
$I_{yy}^{B_1/O_1}$	$9\,667\,065.6\ \mathrm{kg\cdot m^2}$
$I_{zz}^{B_1/O_1}$	$9\,667\,065.6\ \mathrm{kg\cdot m^2}$
${}^{B1}\vec{r}^{J_1/O_1}$	$(25,0,0)$ m
L_{riser}	20.1 m
L_s	82.5 m
L_1	93 m
R_0	18.5 m
h	12.675 m
r	14.04 m

The aerodynamic coefficients of SRB and parachute are given in polynomial form described in Equation 33, with the polynomial coefficients as mentioned in Ibrahim and Engadhl(1974) [8] and tabulated in Table 2.

$$C_{A/N/PM} = \sum_{i=0}^{N} p_i * \alpha^i \tag{33}$$

Table 2: Polynominal Coefficients for Aerodynamics Modelling(Ref: [8])

Coefficients	p_0	p_1	p_2	p_3	p_4
CA_{SRB}	0.6989	$0.1915E^{-8}$	12.56	$-0.1682E^{-7}$	-35.59
CN_{SRB}	$0.2355E^{-9}$	3.645	$-0.8473E^{-8}$	15.20	$0.4432E^{-7}$
CPM_{SRB}	-0.1927	-7.032	-1.114	-12.87	33.24
CA_{PAR}	0.5755	$-0.1637E^{-10}$	-0.8091	$0.3483E^{-10}$	0.4228
CN_{PAR}	$0.2172E^{-11}$	0.3795	$-0.9339E^{-11}$	0.3631	0.0
CPM_{PAR}	$-0.7229E^{-4}$	-0.2742	$0.2576E^{-2}$	-1.271	-0.02333

Fig. 2 shows an exact match between the two formulations, validating the Kane's formulation for the system.

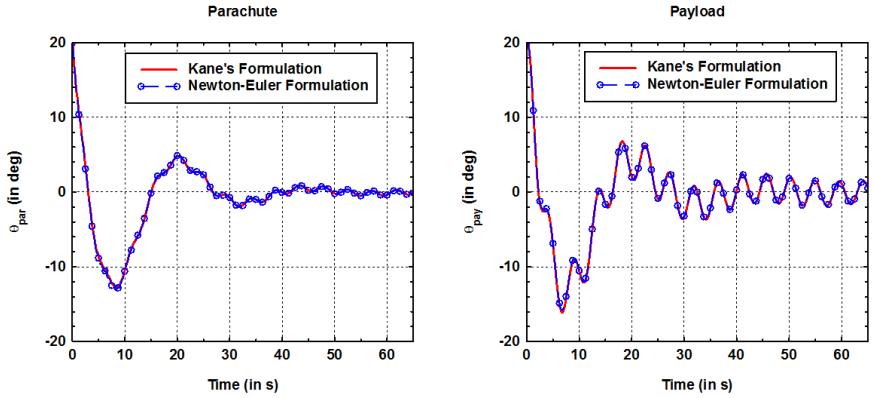

Fig. 2: Pitch Angles of Parachute and Payload (SRB) w.r.t Inertial Frame

Furthermore, end to end simulation from parachute deployment to separation are carried out by modelling the parachute opening force in refeed and disreefed mode, including the apparent mass and fore-body wake effects and considering the effects of mass variations. The additional parameters used for this simulation have been tabulated in Table 3. Considering the canopy shape described in Table 1 and apparent mass computation as mentioned in Equation 29b, α_0 is calculated to be 0.7219587.

The motion of CG's of parachute and payload is shown in Figure 3. During the parachute deployment phase, the payload descends vertically because of gravity and the parachute CG moves in lateral direction owing to the stretching of bridles and suspension lines. When inflation begins, the drag builds up, and stable aerodynamic behaviour ensures the initial lateral movement is corrected by the parachute. Post deployment process, the descend trajectory of the payload is determined by the parachute, where the lateral movement is dependant on the direction of wind, as Parachute drag force acts opposite to the air relative velocity vector. In the current simulation PRPS movement is predominantly in the Eastward direction due to higher Zonal Wind, shown in Figure 4. It is also observed that the pendulum motion under-

Table 3: Additional Parameters used in end to end simulations

Parameters	Value
${}^{B1}\vec{r}^{J_1/O_1}$	$(25,1,0)$ m
m_2	14.594 kg
$t_{stretch}$	1.28 s
$t_{inflation}$	0.63 s
$t_{reef\ cut\ delay}$	7.0 s
$t_{disreef}$	1.4 s
reefing_ratio	0.45

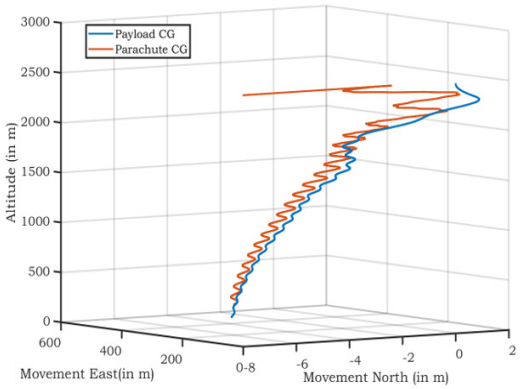

Fig. 3: Trajectories of Payload and Parachute mass centers

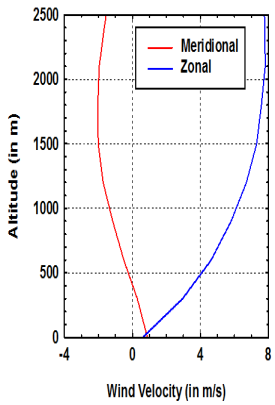

Fig. 4: Simulation Wind

gone by the system is in a plane perpendicular to the dominant motion of the PRPS system. The rotational states of the system from parachute deployment to splashdown is shown in Figure 5. The inertial yaw angle of the payload, has a steady state offset from 0 deg owing to lateral offset in attachment point of riser on the payload, as tabulated in Table 3. The relative joint angles made by riser w.r.t to payload, and parachute w.r.t riser are plotted in Figure 6, which clearly indicates that relative motion between parachute and payload predominantly occurs at the riser-payload joint. The total angle of attack made by the payload and parachute have been shown in Figure 7.

Figure 8 shows the velocity profile and aerodynamic load profile for an end to end parachute simulation. When time is less than $t_{stretch}$, i.e. when the parachute and riser stretches out of payload, aerodynamic load acting on payload is 0 and payload velocity increases due to gravity. Once inflation begins, the velocity reduces attributable to increasing parachute drag, and aerodynamic load first increases as a result of increasing drag of inflating parachute, followed by exponential reduction owing to reduction in dynamic pressure (reducing velocity). Similar profile is observed when disreefing begins. After disreefing, the velocity profile slowly converges to the terminal velocity of descend, but since the simulation considers altitude based density variation, the velocity tends to convergence only.

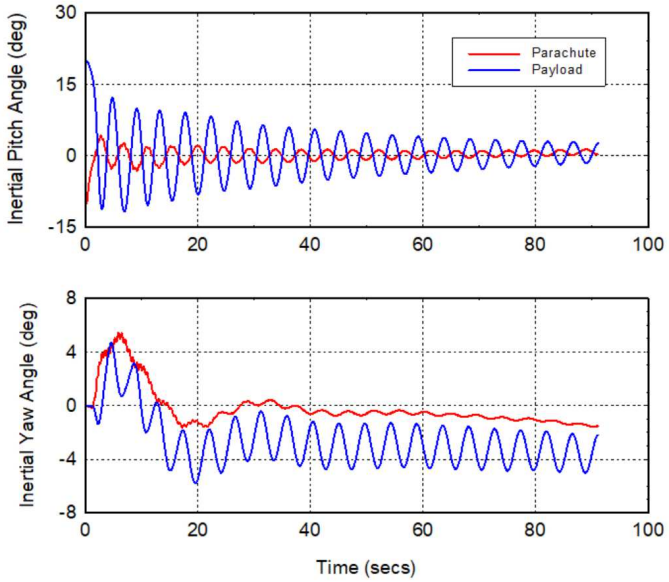

Fig. 5: Pitch Angles of Parachute and Payload w.r.t Inertial Frame (End to End Simulation)

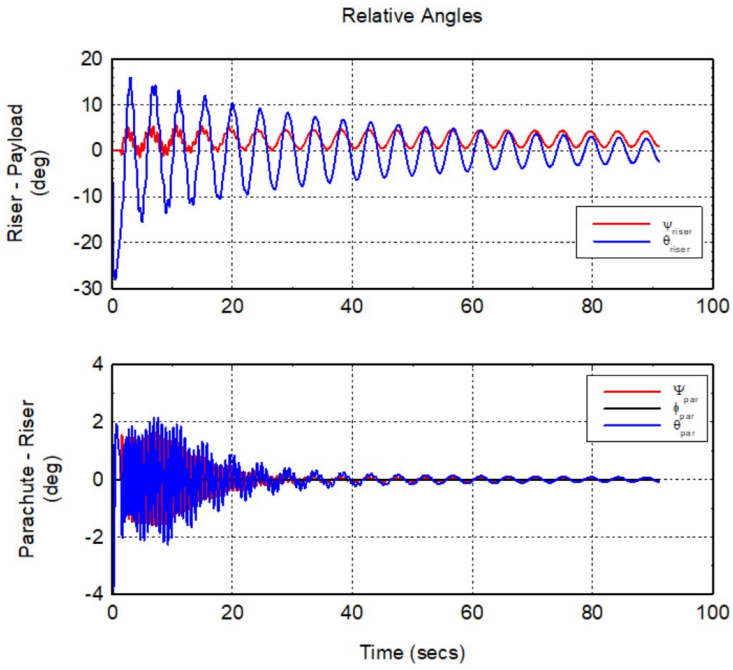

Fig. 6: Relative Joint Angles of Bodies (End to End Simulation)

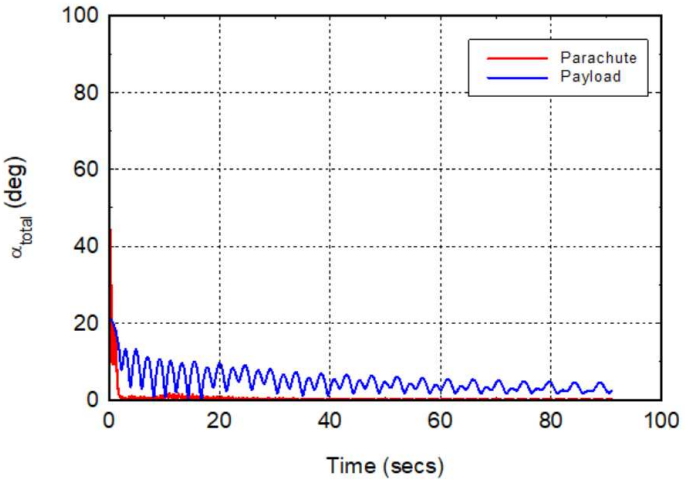

Fig. 7: Total Angle of Attack faced by Parachute and Payload (End to End Simulation)

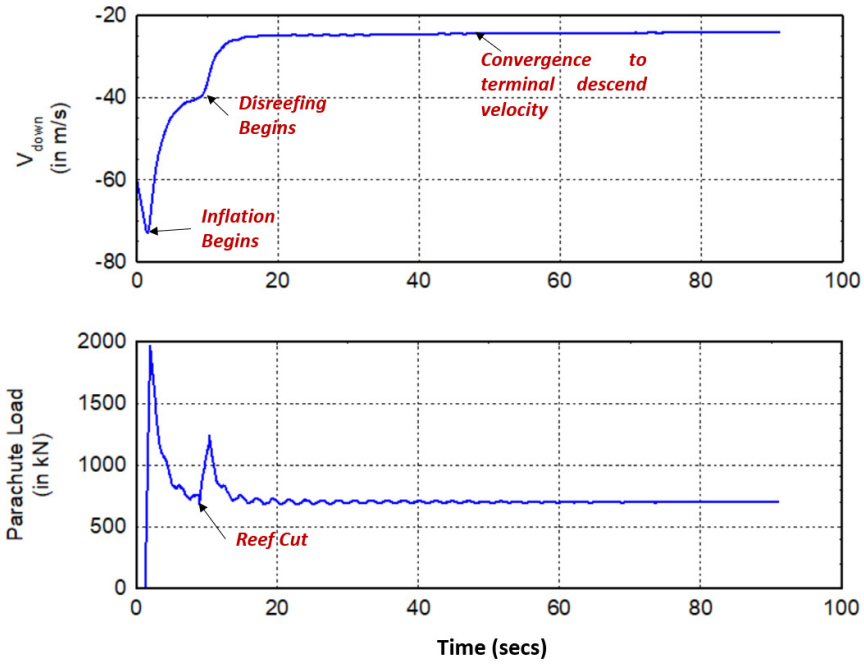

Fig. 8: End-to-end velocity and aerodynamic load profile

5 CONCLUSION

The dynamics of a Single Parachute - Riser - Payload system, consisting of Parachute and Payload sculpted as rigid bodies connected using a elastic riser with non-zero mass, is modelled as 12-DoF system using matrix form of Kane's method. A simplistic reaction thrust based methodology is adopted to model the effects during parachute opening transient due to mass ejection.

The modular matrix formulation of PRPS system ensures that the model can easily be extended to cluster of parachutes, either by considering a single parachute equivalent to cluster (using a cluster coefficient factor to be used in parachute aerodynamics) or by extending the derived velocity, mass-inertia and force matrices for multiple parachutes (considering each parachute as separate bodies and modelling the contact aerodynamics). The fidelity provided by the above model would enable analysis of parachute dynamics especially the cluster interactions leading to various modes during descent, optimize the loads exerted on the payload and understand the effects on the payload trajectory.

References

1. Duan SS, A Comparsion case study of Dynamics Analysis methods used in applied multibody dynamics, American Society for Engineering Education 2006-1859, (2006)
2. Edward J. Fallon, Parachute dynamics and stability analysis of the Queen Match Recovery System, AIAA Paper 91-0879, DOI :10.2514/6.1991-879, URL : https://arc.aiaa.org/doi/abs/10.2514/6.1991-879, (1991)
3. Ge ZM, and Cheng YH, Extended Kanes Equations for Non-Holonomic Variable Mass System, Journal of Applied Mechanics 49(2):429–431, DOI : 10.1115/1.3162105, URL : https://doi.org/10.1115/1.3162105, (1982)
4. Guglieri G, Parachute-Payload SystemFlight Dynamics and Trajectory Simulation, International Journal of Aerospace Engineering 2012, Article ID 182907, DOI : 10.1155/2012/182907, (2012)
5. Heinrich HG and Eckstrom DJ, Velocity Distribution in the Wake of Bodies of Revolution Based on Drag Coefficient, Air Force Flight Dynamics Laboratory Report ASD TDR-62-1103, (1963)
6. Henderson D, Euler angles, quaternions, and transformation matrices – Working relationships, National Aeronautics and Space Administration, Mission Planning and Analysis Division, Washington DC, (1977)
7. Hurtado JE, Analytical Dynamics of Variable-Mass Systems, Journal of Guidance, Control, and Dynamics 41(3):701–709, DOI : 10.2514/1.G002917, URL : https://doi.org/10.2514/1.G002917, (2017)
8. Ibrahim SK, Engdahl RA, Parachute Dynamics and Stability Analysis, NASA-CR-120326, (1974)
9. Kane TR, Levinson DA, Dynamics, theory and applications, McGraw Hill, (1985)
10. Ke P, Yang C, Sun X , Yang S, Novel Algorithm for Simulating the General Parachute-Payload System: Theory and Validation, JOURNAL OF AIRCRAFT 46(1):189-197, DOI : 10.2514/1.34240, URL : https://doi.org/10.2514/1.34240, (2009)
11. Kidane B. : Parachute Drag Area Using Added Mass as Related to Canopy Geometry, 20th AIAA Aerodynamic Decelerator Systems Technology Conference and Seminar, DOI : 10.2514/6.2009-2942, URL : https://arc.aiaa.org/doi/abs/10.2514/6.2009-2942, (2009)
12. Pal, R S , Modelling of helicopter underslung dynamics using kane's method, 6th Conference on Advances in Control and Optimization of Dynamical Systems ACODS, IFAC-PapersOnLine 53(1):536–542, DOI : 10.1016/j.ifacol.2020.06.090, URL : https://www.sciencedirect.com/science/article/pii/S2405896320301099, (2020)
13. Paul J, Nalluveettil SJ; Purushothaman P, Premdas M, Combined Body Dynamics Simulation of Crew Module with Parachutes, 10th National Symposium and Exhibition on Aerospace and Related Mechanisms, (2016)
14. Peterson, Carl W. and Johnson, Donald W., Reductions in Parachute Drag Due to Forebody Wake Effects, Journal of Aircraft 20(1):42-49, DOI : 10.2514/3.44826, URL : https://doi.org/10.2514/3.44826, (1983)
15. Stoneking Eric, Implementation of Kane's Method for a Spacecraft Composed of Multiple Rigid Bodies, AIAA Guidance, Navigation, and Control (GNC) Conference, DOI : 10.2514/6.2013-4649, URL: https://arc.aiaa.org/doi/abs/10.2514/6.2013-4649, (2013)

Conflict of interest

The authors declare that they have no conflict of interest.